

NEOTECTONIC MAP NORWAY AND ADJACENT AREAS

Scale 1:3 000 000
0 50 100 150 200
Kilometres

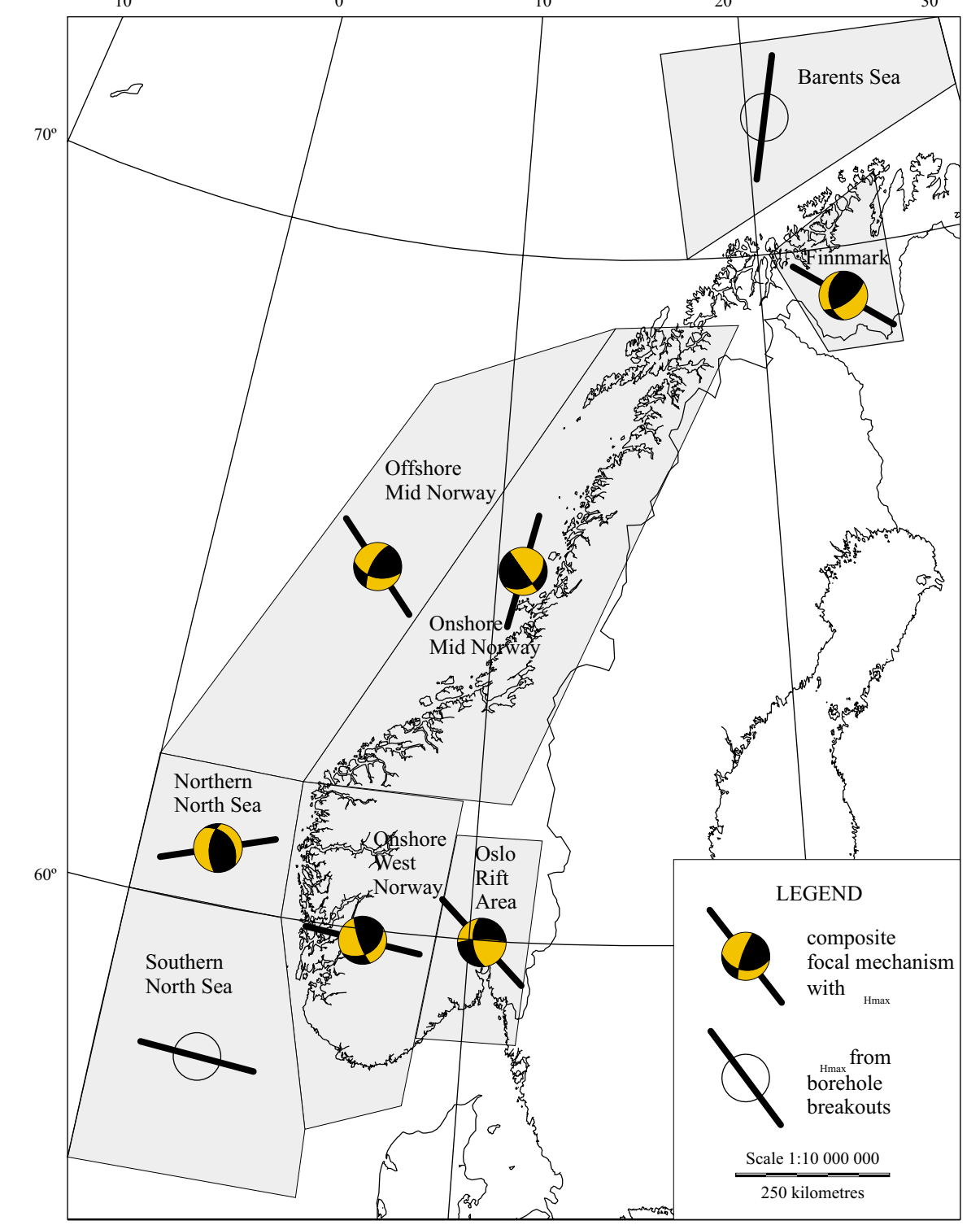
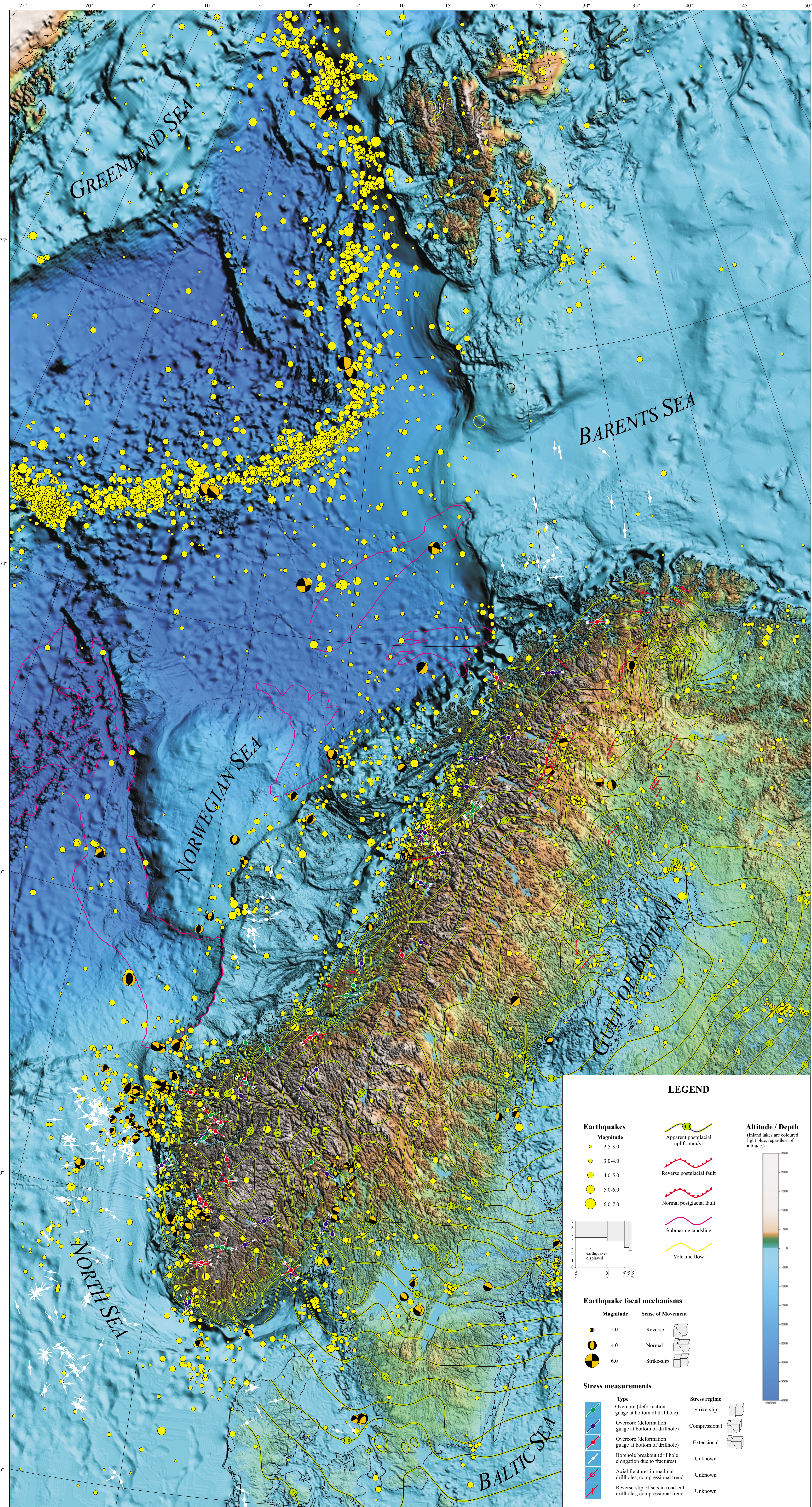


Figure 1. Composite focal mechanism solutions derived from the inversion results for each area. The solution in Finnmark is rotated with regard to the inversion result to reflect the consistent σ_1 direction in the data, as the inversion in this case appears to be unstable due to the low number of solutions in this area. The western Barents Sea and southern North Sea areas are plotted as pure strike-slip solutions, as the only available data there are borehole breakouts with σ_1 values only.

Area	Tectonic regime	Seismic activity level	Focal depth	Mode of faulting	σ_{max}
Northern North Sea	Titanic-Cretaceous off-shore margin	Very high	Deep	Reverse to oblique-reverse	E-W
Offshore Mid Norway	Cenozoic-Pliocene volcanic off-shore margin	High	Deep	Normal to strike-slip	NW-E
Offshore West Norway	Cretaceous thrust belt	High to northern part	Shallow	Normal to strike-slip	SSE-W
Onshore West Norway	Precambrian shield, Thrust belt in the north	High	Shallow	Oblique to the normal to strike-slip	EE-WNW
Oslo Rift Zone	Permian rift	Intermediate	All	Normal (shallow)	E-W
Finnmark	Precambrian basement, Thrust belt near coast	Low	Shallow	Reverse	NW-E
Western Barents Sea	Jurassic-Tertiary rift with later uplift	Very low	Shallow	Reverse	NW-E
Southern North Sea	Titanic-Cretaceous off-shore margin	Low	Deep	Unknown	EE-WNW

Table 1. Summary of the eight areas within which stress inversions have been performed. The seismic activity levels used in the table are relative to Fennoscandia. Focal depths are denoted 'deep' when the bulk of earthquakes occur below 15 km and 'shallow' when most of the earthquakes have depths less than 15 km. Similar principles are applied for stress regimes and stress directions.

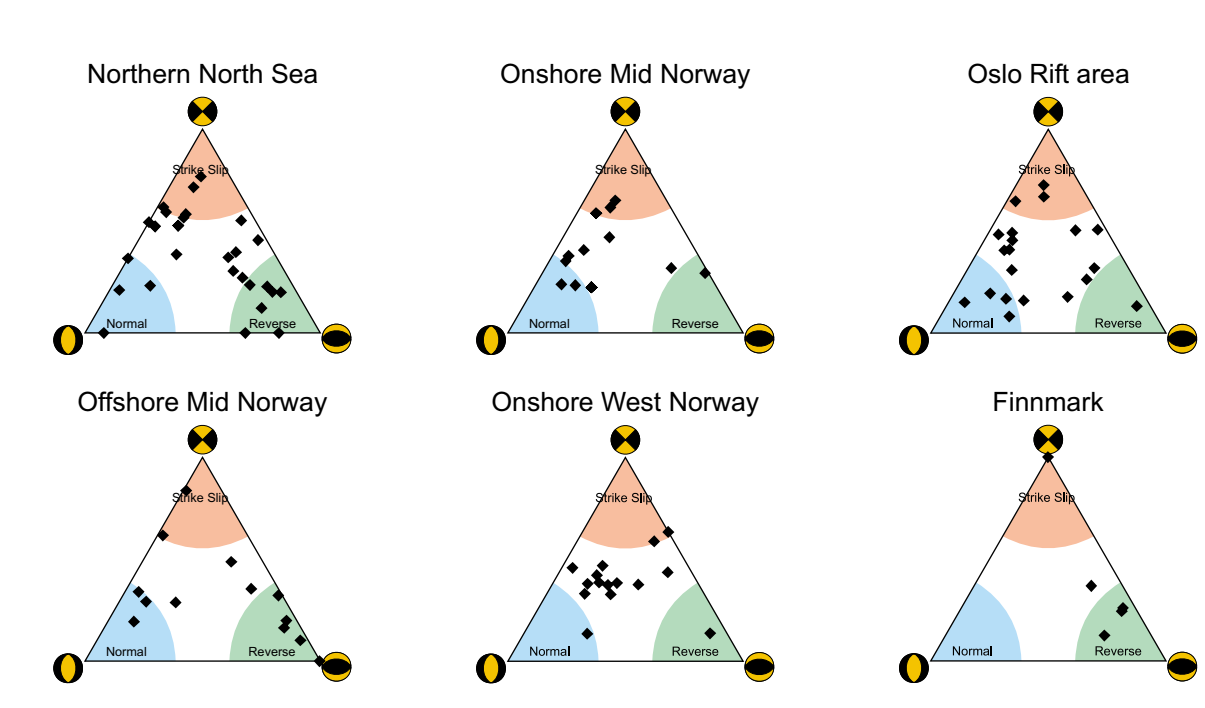


Figure 2. Triangle plots of fault regime distribution of earthquakes focal mechanism solutions. For practical purposes, 'pure' solutions should be contained within the area of each corner. The solutions located elsewhere would thereby be considered to represent oblique faulting.

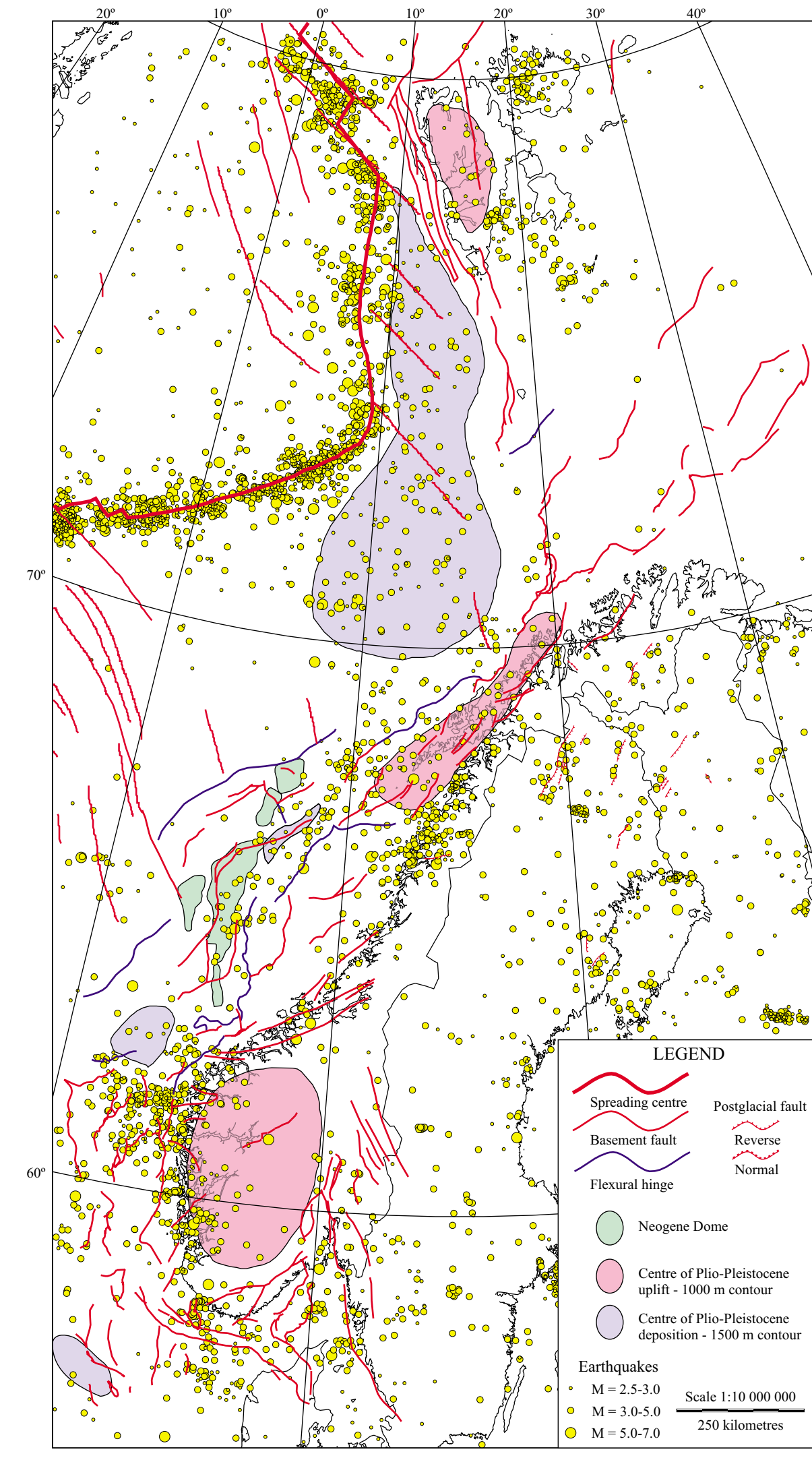


Figure 3. Main basement structures (Brekke 2000), Neogene and Quaternary volcanics and structural elements (Petrová 1977, Skjeltved et al. 1989, Mark & Duncan 1993, Riss 1996, Brekke 2000), postglacial faults (Kjamsuu 1964, Lundquist & Lagerbäck 1976, Olesen 1988, Tøgersbakk & Sollid 1988) and seismicity (NORSAR data) in Norway and adjacent areas. Large submarine landslides (Vøren et al. 1999) are shown on the main map. They are most likely triggered by large earthquakes.

Fault	Country	Length (km)	Max. scarp height (m)	Height (m)	Trend	Type	Moment magnitude	Comment	Reference
Sussekå Fault	Finland	48	5	0.0001	NE-SW	reverse	7.0*		Kjamsuu 1964
Pannilampi/Vesijärvi Fault	Finland	15	12	0.0008	SW-NW	reverse	6.5	two separate sections	Kjamsuu 1964
Vaalajärvi Fault	Finland	6	2	0.0003	NW-SE	??	6.0		Kjamsuu 1964
Präve Fault	Sweden	150	13	0.0001	NE-SW	reverse	7.6		Lundquist & Lagerbäck 1976
Lainio-Saigvarra Fault	Sweden	55	30	0.0005	NE-SW	reverse	7.1		Lagerbäck 1979
Merajärvi Fault	Sweden	9	18	0.0002	NE-SW	reverse	6.3		Lagerbäck 1979
Pantimys Fault	Sweden	18	2	0.0001	NE-SW	reverse	6.5		Lagerbäck 1979
Lansjöv Fault	Sweden	50	22	0.0004	NE-SW	reverse	7.1		Lagerbäck 1979
Barrnäs-Barrnäs Fault	Sweden	60	< 10	0.0002	NE-SW	??	7.1	two separate sections	Lagerbäck 1979
Sauegrava Fault	Norway	80	7	0.0001	NE-SW	reverse	7.3	three separate sections	Olesen 1988
Nordmannvik-dalen Fault	Norway	3	1	0.0003	NW-SE	normal	5.7		Tøgersbakk & Sollid 1988

Table 2. Summary of properties of the documented postglacial faults within the Lapland province. The major faults are NE-SW trending reverse faults and occur within a 400 x 400 km large area in northern Fennoscandia. The Nordmannvik-dalen and Vaalajärvi faults are minor faults trending perpendicular to the reverse faults. The former is a normal fault and the latter is a potential normal fault. The scarp height/length ratio is generally less than 0.01. The Merajöv Fault has a scarp height/length ratio of 0.002. * Moment magnitudes calculated from fault length using formulas from Wells & Coppersmith (1994).

MAP DESCRIPTION
The mapped area includes Norway, Denmark, Sweden, northern Finland, Svalbard and part of the North Sea, the Norwegian Sea, the Greenland Sea and the western Barents Sea.
Information on contemporary crustal uplift, seismicity and rock stress in addition to Neogene domes, depocentres and volcanic rocks, and postglacial faults has been compiled in the present 1:3 million map and in Figure 3.

- Regional neotectonics**
There are seven major components of Neogene tectonics in the map area:
- Oceanic spreading along the Molins and Knipovich Ridges in the Norwegian Sea.
 - Uplift and exhumation of the mainland and the Barents Sea.
 - Neogene (Mid Miocene?) reactivation of domes, arches and faults offshore Mid-Norway (many of them originally formed in the Eocene).
 - Neogene volcanism on northern Spitzbergen and the western Barents Sea.
 - The offshore subsidence and deposition of large Pliocene-Pleistocene prograding wedges.
 - The Lapland province of reverse postglacial faults.
 - Glaciation/deglaciation cycles throughout the Late Neogene and the Quaternary.

The six former components are included on the neotectonic map and in Figure 3. It is still uncertain which of these elements are correlated and how they may be linked genetically.
In general, Neogene tectonics seems to be related both to the ridge-push force associated with the rifting along the Molins and Knipovich Ridges, and to the forces set up by glacial loading and unloading. However, their relative significance is not known. As an example, it is still an open question whether the observed postglacial faults are caused by the ridge-push force or by the major strain release immediately following glacial unloading, or a possible combination of these effects. Since the formation of the offshore domes and arches was initiated in Eocene, it is natural to relate these features to tectonic forces related to the plate boundary. The south Norway mountain plateau and the Lofoten area seem to be areas of recent vertical movement (Figure 3). Riss (1996) suggested that the Pliocene uplift was constructed in a tectonic phase during the last 1 Ma correlating with change in glaciation intensity and cyclicity and modification of sedimentation and ice loads. Stuevold et al. (1992) and Vågenes & Amundsen (1993) advocate that the intraplate deformation is an effect of a deep-seated thermal source. The two areas of Plio-Pleistocene uplift occur in regions with mantle material with anomalous low seismic velocity (Banister et al. 1991). The present uplift of these two areas can not be attributed to postglacial rebound alone (Fjeldskaar et al. in press) and consequently indicates that the mechanism that caused the Plio-Pleistocene uplift, is still active.

The Lapland postglacial fault province (Table 2) occurs in northern Norway (Kjamsuu 1964, Kuivamäki et al. 1998), northern Norway (Olesen 1988, Tøgersbakk & Sollid 1988) and northern Sweden (Lundqvist & Lagerbäck 1976, Lagerbäck 1979) within a 400 x 400 km large area. The Präve Fault is up to 150 km in length. The Lainio-Saigvarra Fault has an escarpment of 30 m in height. The major faults are NE-SW trending reverse faults while the two minor faults, the Nordmannvik-dalen and Vaalajärvi faults, have a NW-SSE trend, that is perpendicular to the trend of the reverse faults. The Nordmannvik-dalen fault in northern Troms is a normal fault (Djehs et al. in press). The dip of the parallel Vaalajärvi Fault in northern Finland is not known, but recent trenching indicates a normal fault (Kuivamäki et al. in press).

Seismicity and crustal stress
The earthquake catalogue was produced by NORSAR, and contains modern and historical events from 1750 to 1999. For the period 1750 to 1890, only earthquakes with magnitudes greater than or equal to 4.5 are reported. For the period 1891 to 1965, only earthquakes with magnitudes greater than or equal to 4.0 are reported. For the period 1966 to 1985, only earthquakes with magnitudes greater than or equal to 3.0 are reported. For the period from 1986 to 1999, only earthquakes with magnitudes greater than or equal to 2.5 are reported. The seismicity of Norway and adjacent areas is intermediate in level, and even though it is the highest of northwestern Europe it is still lower than in many other stable continental (intraplate) regions (Byrkjeland et al. 2000).
The stress indicators from 130 earthquakes and various in situ data (Hicks et al. submitted) are included on the main map. These data are summarised in Figure 1 and Table 1, where the data within each of the areas are inverted for the best fitting stress tensor. Modes of faulting for individual regions are displayed as triangle plots in Figure 2. The results support the earlier finding (Bangum et al. 1991; Lindholm et al. 2000) that the maximum horizontal compressive stress complies with the expected NW-SE trends of the ridge push force. Additional data from road-cut drillholes (Roberts in press) are consistent with the regional pattern.

There are important deviations, however, and notably so in the Nordland region where data from the NEONOR project have revealed an apparent 90° rotation of the direction of maximum horizontal stress as inferred from shallow earthquakes in the region (Hicks et al. in press). The same phenomenon is seen also, albeit less pronounced, in the Sørgraben-Tananger Spur region (Lindholm et al. 2000). However, in Nordland this reversal is connected predominantly to shallow normal-faulting earthquakes, indicating that the significant stress component is extensional and coast-perpendicular, which, when taken together with the fact that this is a region of maximum crustal uplift gradient, points to postglacial rebound as a potentially important source of stress in this region. More local stress perturbations, however, are still likely to be involved.

In general, in situ stress directions comply with those inferred from earthquakes (Fejerskov et al. 1995), but with important deviations in the western Barents Sea where the ridge push force should be expected to be different in both direction and strength, reflecting the changes in direction, morphology and rheology as one moves from the Molins Ridge and into the Knipovich Ridge. In the southern North Sea, however, from where there are no earthquake focal mechanisms, the NW-SE trend is maintained, in contrast to the Central Graben where the in situ stress directions are more or less random and expected to be related to a difference in the ability of the sedimentary rocks in the two regions to support regional stress propagation.

Present rate of uplift
The present rate of uplift in Fennoscandia was calculated using data from tide-gauges, precise levelling, GPS and gravity measurements. Uplift rates calculated from repeated precise levelling along roads throughout Norway, Sweden and Finland make up the bulk of the data. Levelling results from the northern part of Finland have been used, together with the first, second, and a few lines from the third precision levelling of Sweden. Data from all available Norwegian precision levelling lines were used, including the lines measured by surveyors from the Norwegian Railways (J. Danielsen, pers. comm. 1999). The levelling lines are tied to tide-gauges along the coast. Additional tide gauge records from around the Baltic Sea (Ekman 1998) helped constrain the regional uplift pattern. Between 1966 and 1984, repeated precise gravity measurements were performed on three lines across Norway, Sweden and Finland to determine the rate of uplift (Miklösen et al. 1986). Permanent GPS stations located in Sweden and Finland have also provided measurements of uplift rate (Ekman 1998).
Uplift data from all sources were combined and gridded using a minimum curvature method. The crustal uplift contours are mainly influenced by the isostatic readjustment caused by the removal of approximately 3000 m of ice in central Fennoscandia since the glacial maximum.

Although data are scarce, it is evident that there are local disturbances in the uplift pattern which may be caused by other tectonic forces or by stress concentration along zones of weakness (Fjeldskaar et al. in press). The rate of uplift is close to zero along the Norwegian coast, increasing to more than 8 mm/yr in central parts of the Gulf of Bothnia.

References
Banister, S.C., Road, B.O. & Husebye, E.S. 1991. Tomographic estimates of sub-Moho seismic velocities in Fennoscandia and structural implications. *Tectonophysics* 189, 37-53.
Brekke, H. 2000. The tectonic evolution of the Norwegian Sea continental margin, with emphasis on the Vøring and Møre basins. *Geological Society of London Special Publication* 167, 327-378.
Bangum, H., Aluok, A., Kvamme, L.B. & Hansen, R.A. 1991. Seismicity and seismotectonics of Norway and nearby continental shelf areas. *Journal of Geophysical Research* 96, 2249-2265.
Byrkjeland, U., Bangum, H. & Eilidson, O. 2000. Seismotectonics of the Norwegian continental margin. *Journal of Geophysical Research* 105, 6221-6234.
Djehs, J.D., Olesen, O., Olesen, L. & Blåka, L.H. (in press). Neotectonic faulting in northern Norway: the Sauegrava and Nordmannvik-dalen postglacial faults. *Quaternary Science Reviews*.
Ekman, M. 1998. Recent postglacial rebound of Fennoscandia: a short review and some numerical results. *Geotectonics Forum* 3, 383-392.
Fjeldskaar, W., Lindholm, C., Djehs, J.F. & Fjeldskaar, C. (in press). Post-glacial uplift, neotectonics and seismicity in Fennoscandia. *Quaternary Science Reviews*.
Fejerskov, M., Lindholm, C.D., Myrberg, A. & Bangum, H. 1995. In situ rock stress pattern on the Norwegian Continental Shelf and mid-Norway. In: Fjeldskaar, M. & Myrberg, A.M. (eds.), *Proceedings of the Workshop: Rock Stress in the North Sea*, University of Tromsø, Norway, 191-201.
Hicks, E.C., Bangum, H. & Lindholm, C.D. (submitted). Stress inversions of earthquake focal mechanism solutions from onshore and offshore Norway. *Norwegian Geological Tidskrift*.
Hicks, E.C., Bangum, H. & Lindholm, C.D. (in press). Seismic activity, inferred crustal stresses and seismotectonics in the Rana region, Northern Norway. *Quaternary Science Reviews*.
Kuivamäki, A., Paananen, M. & Vuorela, P. (in press). New structural observations of the Vaalajärvi and Rautajärvi postglacial faults in Finland. *Journal of Geophysical Research of Finland, Nuclear Waste and Environment, Report 197-102*.
Kjamsuu, R. 1964. Nuoreista sirroksista Lapissa. Summary: Recent faults in Lapland. *Geologiska Föreningsningens Årsskrift* 86, 36-36.
Lagerbäck, R. 1979. Neotectonic structures in northern Sweden. *Geologiska Föreningsningens Årsskrift* 100 (1978), 271-278.
Lindholm, C.D., Bangum, H., Hicks, E.C. & Villagran, M. 2000. Crustal stress and tectonics in the Norwegian region determined from earthquake focal mechanisms. In: Burg and al. (eds.) *Dynamics of the Norwegian Margin*. Geological Society of London Special Publication 167, 429-439.
Lundqvist, J. & Lagerbäck, R. 1976. The Präve Fault: A late-glacial fault in the Precambrian of Swedish Lapland. *Geologiska Föreningsningens Årsskrift* 98, 45-51.
Miklösen, J., Ekman, M., Mieland, A. & Remmer, O. 1986. The Fennoscandian land uplift gravity lines 1966-1984. *Reports of the Finnish Geodetic Institute* 85, 159 pp.
Mark, M.B. & Duncan, R.A. 1993. Late Pliocene basaltic volcanism on the Western Barents Shelf margin: implications from petrology and 40Ar-39Ar dating of volcanoclastic debris from a subglacial drill core. *Journal of Geophysical Research* 98, 209-225.
Olesen, O. 1988. The Sauegrava Fault, evidence of neotectonics in the Precambrian of Finnmark, northern Norway. *Norsk Geologisk Tidsskrift* 68, 107-118.
Prest, T. 1977. Cenozoic palaeogeography and tectonics of Spitzbergen. *Norsk Polarvitenskaplig Tidsskrift* 1977, 129-143.
Riss, F. 1996. Quantification of Cenozoic vertical movements of Scandinavia by correlation of morphological surfaces with offshore data. *Global and Planetary Change* 12, 331-357.
Roberts, D. (in press). Reverse-slip offsets and axial fractures in road-cut boreholes in the Caledonides in Finnmark, northern Norway: neotectonic stress orientation indicators. *Quaternary Science Reviews*.
Skjeltved, B.-L., Amundsen, H.E.F., Ørby, S.V., Griffin, W.L. & Gjelsvik, T. 1989. A primitive alkali basaltic stratovolcano and associated igneous centres, northwestern Spitzbergen: volcanology and tectonic significance. *Journal of Volcanology and Geothermal Research* 37, 1-19.
Stuevold, L.M., Skjeltved, B.-L. & Eilidson, O. 1992. Post-Cretaceous uplift events on the Vøring continental margin. *Geology* 20, 919-922.
Tøgersbakk, J. & Sollid, J.L. 1988. Klif og kvartærgeologi og geomorfologi i SO 000, 1634. Geografisk institutt, Universitetet i Oslo.
Vøren, T.O., Labeyrie, J.S., Blumne, F., Dowdell, J.A., Keyser, N.H., Miesner, J., Ramberg, J. & Werner, F. 1999. The Norwegian-Greenland Sea continental margin: Late Quaternary sedimentary processes and environment. In: O.J. Martinsen & T. Dreyer (eds.), *Sedimentary environment offshore Norway*. Polarcenter, Tromsø, 201-204.
Vågenes, E. & Amundsen, H.E.F. 1993. Late Cenozoic uplift and volcanism on Spitzbergen - caused by mantle convection. *Geology* 21, 251-254.
Wells, D.L. & Coppersmith, K.J. 1994. Empirical relationships among magnitudes, rupture length, rupture area and surface displacement. *Bulletin of the Seismological Society of America* 82, 1704-1714.

Reference to the map:
Djehs, J.F., Olesen, O., Bangum, H., Hicks, E.C., Lindholm, C.D. & Riss, F. 2000. Neotectonic map: Norway and adjacent areas. Geological Survey of Norway

Projection: Transverse Mercator
Longitude of central meridian: 15° 0' 0"
Latitude of origin: 0° 0' 0"
Scale factor at central meridian: 1.0
Datum: WGS84

Data Sources:
Geological Survey of Norway
Geological Survey of Sweden
Geological Survey of Finland
Norwegian Mapping Authority
NORSAR
Norwegian Petroleum Directorate
Finnish Geodetic Institute
National Land Survey of Sweden
National Survey and Cadastre, Denmark
University of Bergen
Uppsala University
University of Helsinki
Norwegian University of Science and Technology
SINTEF

Project Contributors:
J. Adams, E. Anda, L. H. Blåka, L. Bockmann, H. Brekke, A. Braathen, H. Bangum, R. Bøe, J. F. Djehs, J. I. Falade, S. Fanavoll, I. Fjeldskaar, W. Fjeldskaar, R. H. Gabrielsen, P. J. Goldsmith, I. Grimstvedt, E. C. Hicks, B. O. Hilmo, R. Hunsdale, I. J. Hågenesen, M. R. Karpuz, F. Krüger, E. Johannsson, T. Klemetsrud, P. Pantimys, S. D. Lindholm, O. Longva, E. Murring, A. Myrberg, O. Olesen, L. Olesen, G. Richter, F. Riss, L. Rise, D. Roberts, J. S. Romning, S. Schweitzer, M. G. Shalby, I. Skogeth, K. Sletten, A. Sylvestre, M. Thoresen & J. F. Tommessen